

Probing Non-leptonic Two-body Decays of B_c meson

Hui-feng Fu^a, Yue Jiang^a, C. S. Kim^{b*}, Guo-Li Wang^{a†}

^a *Department of Physics, Harbin Institute of Technology, Harbin, 150001, China*

^b *Department of Physics & IPAP, Yonsei University, Seoul 120-749, South Korea*

Abstract

Rates and CP asymmetries of the non-leptonic two-body decay of B_c are calculated based on the low energy effective Hamiltonian. We concentrate on such b quark decays of the processes with 0^- and 1^- S-wave particles and/or 0^+ and 1^+ P-wave particles in the final states. The Salpeter method, which is the relativistic instantaneous approximation of the original Bethe-Salpeter equation, is used to derive hadron transition matrix elements. Based on the calculation, it is found that the best decay channels to observe CP violation are $B_c^- \rightarrow \eta_c + D^-(D_0^{*-})$, which need about $\sim 10^7$ B_c events in experiment. Decays to $\eta_c + D^{*-}(D_s^-)$, $h_c + D^-(D^{*-})(D_0^{*-})$, $J/\Psi + D^{*-}$ are also hopeful channels.

1 Introduction

The discovery of the B_c meson [1] has provided a new valuable window for studying the heavy quark dynamics and CP violation. Studies on the B_c decays and their CP asymmetries have drawn much attention in accordance with the coming LHC-b experiment. Since the LHC-b is expected to produce around 5×10^{10} B_c events per year [2] and to provide detailed information about the B_c meson, it becomes more and more strongly relevant to investigate B_c decay and its CP violation in detail.

There are two major reasons which make the B_c meson special. The first is that it is unique to have two heavy-flavored quarks, composed of a charm quark (anti-quark) and a bottom anti-quark (quark). The other heavy quark in the Standard Model, *i.e.* the top quark, cannot form a hadron because of its too short lifetime to be hadronized. The second reason is that it can decay only via weak interactions, since the pure strong and electromagnetic interacting processes conserve flavors, and the B_c meson, as the ground state of $c\bar{b}$ system, is below the BD mesons decay threshold. Due to these properties, the B_c meson has a long lifetime and rich decay channels.

The quark diagrammatic approach has established and well developed for meson decays. In the approach, there are five diagrams contributing to B_c decays: the color-favored tree diagram,

* cskim@yonsei.ac.kr

† gl_wang@hit.edu.cn

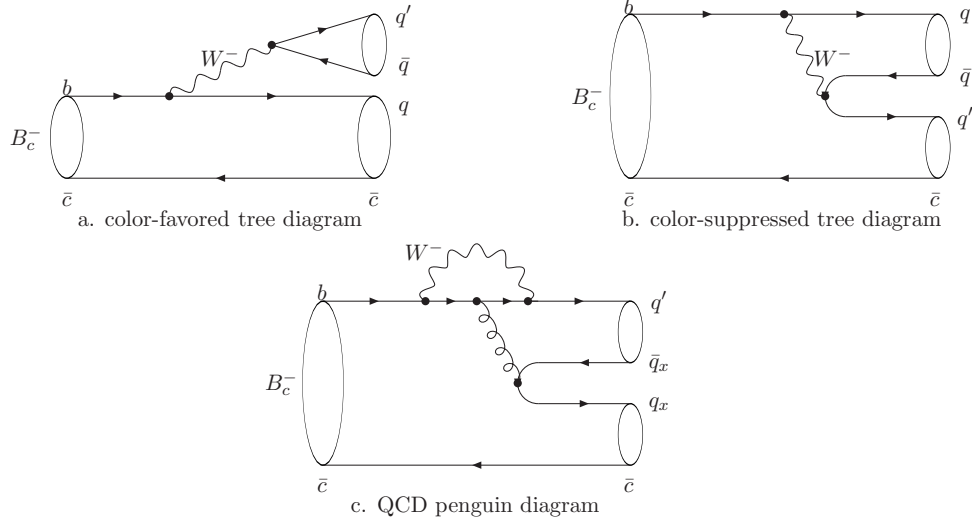


Figure 1: The tree and QCD penguin diagrams of non-leptonic two-body B_c decay. $q = u$ or c and $q' = s$ or d ; q_x ranges from u, d, s to c .

the color-suppressed tree diagram, the time-like penguin diagram, the annihilation diagram and the space-like penguin diagram. The direct CP violation requires at least two diagrams with different weak and strong phases contributing to the relevant process. The weak phases come from CKM matrix elements within the Standard Model, and the strong phases arise from final state interactions including penguin effects (hard strong phases), which can be estimated perturbatively, as well as rescattering effects (soft strong phases), which cannot be estimated solidly now. Therefore, we only discuss penguin effects for the generation of strong phases in this paper.

Non-leptonic two-body decays can play an important role for exploring the direct CP violation. So far many works on non-leptonic B_c decays and their CP violations have been investigated [3]–[16]. But in those works CP violation of the channels with P-wave final states has not been considered. Here we are going to concentrate on such non-leptonic two-body decay channels that may have direct CP asymmetries: We study the $b(\bar{b})$ quark decays with final states involving not only pseudoscalar (0^-) and vector (1^-) particles but also 0^+ and 1^+ P-wave particles. Since the contributions from the annihilation diagram and space-like penguin diagram are helicity suppressed, these two type diagrams are ignored in our calculation. Furthermore, the electroweak penguin effects are much smaller compared to the QCD penguin effects, so only the QCD penguin effects are considered here. Therefore, only the two tree diagrams and the time-like QCD penguin diagrams are fully considered (see Fig. 1). The CP asymmetries arise from the interference between the penguin diagrams and tree diagrams or/and the penguin diagrams themselves.

In our calculation the factorization approach is assumed and the Salpeter method is used: With the factorization approach, the amplitude can be expressed by the products of form factors and decay constants. The Salpeter method is used to calculate the form factors at finite recoils. In doing so, a relativistic treatment is needed especially for $B_c \rightarrow D/D_s + X$ processes, since the D/D_s mesons are bound states composed of a heavy and a light quark and the relativistic corrections to such particles may be noticeable. It is well known that the Bethe-Salpeter (B-S) equation is a relativistic two-body wave equation and the Salpeter method is just the instantaneous approximation of the B-S equation. With the Salpeter equation and well defined wave functions, we can treat the bound states relativistically. Therefore, in our calculations the relativistic corrections are also systematically covered.

The remainder of this paper is organized as follows: In section 2, the factorization approach based on the low energy effective Hamiltonian is introduced to evaluate the decay amplitudes. Section 3 contains a brief review on the Salpeter method and our model calculation. Section 4 is devoted to numerical results and discussions.

2 Nonleptonic two-body decay and its CP asymmetry of B_c

In weak decay analysis, the basic starting point is the effective weak Hamiltonian [17], which in the case of $b \rightarrow u$ decay is

$$\mathcal{H}_{\text{eff}}(\Delta B = 1) = \frac{G_F}{\sqrt{2}} \left\{ V_{ub}V_{uq'}^*(C_1Q_1^u + C_2Q_2^u) - \frac{\alpha_s(m_b)}{8\pi} \left(\sum_{i=u}^{c,t} V_{ib}V_{iq'}^* I_i \right) \left(-\frac{Q_3}{N_c} + Q_4 - \frac{Q_5}{N_c} + Q_6 \right) \right\}, \quad (1)$$

where Q_1^u, Q_2^u are the tree operators in $b \rightarrow u$ decay, which would be replaced by Q_1^c, Q_2^c in $b \rightarrow c$ decay. Q_3, Q_4, Q_5 and Q_6 are the QCD penguin operators. All these local operators are

$$\begin{aligned} Q_1^u &= (\bar{q}'_\alpha u_\beta)_{V-A} (\bar{u}_\beta b_\alpha)_{V-A}, \\ Q_2^u &= (\bar{q}'_\alpha u_\alpha)_{V-A} (\bar{u}_\beta b_\beta)_{V-A}, \\ Q_1^c &= (\bar{q}'_\alpha c_\beta)_{V-A} (\bar{c}_\beta b_\alpha)_{V-A}, \\ Q_2^c &= (\bar{q}'_\alpha c_\alpha)_{V-A} (\bar{c}_\beta b_\beta)_{V-A}, \\ Q_3 &= (\bar{q}'_\alpha b_\alpha)_{V-A} \sum_{q_x} (\bar{q}_{x\beta} q_{x\beta})_{V-A}, \\ Q_4 &= (\bar{q}'_\alpha b_\beta)_{V-A} \sum_{q_x} (\bar{q}_{x\beta} q_{x\alpha})_{V-A}, \\ Q_5 &= (\bar{q}'_\alpha b_\alpha)_{V-A} \sum_{q_x} (\bar{q}_{x\beta} q_{x\beta})_{V+A}, \\ Q_6 &= (\bar{q}'_\alpha b_\beta)_{V-A} \sum_{q_x} (\bar{q}_{x\beta} q_{x\alpha})_{V+A}, \end{aligned} \quad (2)$$

where $q' = s$ or d , and the subscript α, β are color indices. q_x ranges from u, d, s to c . The operator $(\bar{\psi}_{1\alpha}\psi_{2\beta})_{V-A} \equiv \bar{\psi}_{1\alpha}\gamma^\mu(1 - \gamma_5)\psi_{2\beta}$, and the operators with $V + A$ represent for the right-handed currents. In Eq. (1), C_1, C_2 in front of the tree operators are Wilson coefficients. $N_c = 3$ is the number of colors and $V_{qq'}$ are the CKM matrix elements. $I_i (i = u, c, t)$ are the QCD loop integrals [4, 18]:

$$I_{u,c} = -4 \int_0^1 x(1-x) \ln \frac{m_{u,c} - k^2 x(1-x)}{m_W^2} dx, \quad (3)$$

$$I_t = -\frac{1}{9} + \frac{1}{6} \int_0^1 \frac{(1-x)[(2 + m_t^2/m_W^2)(1-x)(2+x) + 12x]}{m_t^2/m_W^2 + (1 - m_t^2/m_W^2)x} dx, \quad (4)$$

where $m_{u,c,t}$ are the current quark masses; k is the momentum of the gluon in penguin diagram, see Fig 1 c. Usually one takes a certain value of k^2 in the range $[\frac{1}{4}m_b^2, \frac{1}{2}m_b^2]$ or $[0, m_b^2]$ [19]. As argued by the authors in Ref. [6], it is not a good choice to pick up a fixed value of k^2 for all decay modes. In this work, we follow the simple kinematic picture presented in Ref. [6] for the value of k^2 . One can see from Fig. 1 c, as c quark being a spectator, the relation of the momenta among the quarks and gluon $p_b = k + p_{q'} = p_{q_x} + p_{\bar{q}_x} + p_{q'}$ are hold. Since the q' quark and the \bar{q}_x anti-quark form a meson, noted as X , the momentum of X satisfies $p_X = p_{\bar{q}_x} + p_{q'}$. With these relations one can get $k^2 = m_b^2 + m_{q'}^2 - 2E_b E_{q'} + 2|\vec{p}_b||\vec{p}_{q'}|\cos(\phi)$, where ϕ is the angle between the 3-momenta of b quark \vec{p}_b and q' quark $\vec{p}_{q'}$ in the rest frame of the X meson. Since the angle ϕ is unknown, we use the averaged value \bar{k}^2 to evaluate the loop-integral functions. After all, one get

$$\frac{\bar{k}^2}{m_b^2} = \frac{1}{2}(1 + (m_{\bar{q}_x}^2 - m_{q'}^2)(1 - \frac{m_{\bar{q}_x}^2}{m_X^2})/m_X^2 + (m_{q'}^2 + 2m_{\bar{q}_x}^2 - m_X^2)/m_b^2). \quad (5)$$

Now we turn to evaluate the decay amplitudes in factorization approach [20, 21] and take the $B_c^- \rightarrow \eta_c + D^-$ channel as an example. The decay amplitude of this process is $\langle \eta_c, D^- | \mathcal{H}_{\text{eff}} | B_c^- \rangle$. First, consider the color-favored tree diagram (see Fig. 1 a), where the tree operators Q_1^c and Q_2^c contribute. Using the Fierz rearrangement

$$(\bar{\Psi}_1\Psi_2)_{V-A}(\bar{\Psi}_3\Psi_4)_{V-A} = (\bar{\Psi}_1\Psi_4)_{V-A}(\bar{\Psi}_3\Psi_2)_{V-A}, \quad (6)$$

$$(\bar{\Psi}_{1\alpha}\Psi_{2\beta})_{V-A}(\bar{\Psi}_{3\beta}\Psi_{4\alpha})_{V-A} = \frac{1}{N_c}(\bar{\Psi}_{1\alpha}\Psi_{2\alpha})_{V-A}(\bar{\Psi}_{3\beta}\Psi_{4\beta})_{V-A} + \text{Octet}, \quad (7)$$

$$(\bar{\Psi}_1\Psi_2)_{V-A}(\bar{\Psi}_3\Psi_4)_{V+A} = -2(\bar{\Psi}_1\Psi_4)_{S+P}(\bar{\Psi}_3\Psi_2)_{S-P}, \quad (8)$$

where the ‘‘Octet’’ is the color-octet term which does not contribute in the factorization approach. One can get the amplitude of the color-favored tree diagram

$$\frac{G_F}{\sqrt{2}} V_{cb} V_{cd}^* a_1 \langle \eta_c | (\bar{c}b)_{V-A} | B_c^- \rangle \langle D^- | (\bar{d}c)_{V-A} | 0 \rangle,$$

where $a_1 \equiv \frac{C_1}{N_c} + C_2$. The other two amplitudes (corresponding to Fig. 1 b and Fig. 1 c) can be obtained in the same way. In the penguin diagram, we will encounter the term $(\bar{d}c)_{S+P}(\bar{c}b)_{S-P}$,

where $(\bar{q}_1 q_2)_{S\pm P} = (\bar{q}_1(1 \pm \gamma_5)q_2)$. To evaluate these terms, we use the equation of motion, which gives

$$\langle P' | \bar{q}_1 q_2 | P \rangle = \frac{P^\mu - P'^\mu}{m_1 - m_2} \langle P' | \bar{q}_1 \gamma_\mu q_2 | P \rangle, \quad (9)$$

$$\langle P' | \bar{q}_1 \gamma_5 q_2 | P \rangle = \frac{P^\mu - P'^\mu}{m_1 + m_2} \langle P' | \bar{q}_1 \gamma_\mu \gamma_5 q_2 | P \rangle, \quad (10)$$

where P and P' are the momenta of initial and final states respectively and m_1, m_2 are the current quark masses. Now we can write the decay amplitude of the process

$$\begin{aligned} \mathcal{M}(B_c^- \rightarrow \eta_c + D^-) = & \frac{G_F}{\sqrt{2}} \left\{ \left[V_{cb} V_{cd}^* a_1 - \frac{\alpha_s(m_b)}{8\pi} (V_{ub} V_{ud}^* I_{ut} + V_{cb} V_{cd}^* I_{ct}) \left(1 - \frac{1}{N_c^2}\right) \times \right. \right. \\ & \times \left. \left(1 + \frac{2M_{D^-}^2}{(m_b - m_c)(m_d + m_c)}\right) \right] \langle \eta_c | (\bar{c}b)_{V-A} | B_c^- \rangle \langle D^- | (\bar{d}c)_{V-A} | 0 \rangle \\ & \left. + V_{cb} V_{cd}^* a_2 \langle D^- | (\bar{d}b)_{V-A} | B_c^- \rangle \langle \eta_c | (\bar{d}c)_{V-A} | 0 \rangle \right\}, \quad (11) \end{aligned}$$

where $a_2 \equiv \frac{C_2}{N_c} + C_1$ and $I_{ut} \equiv I_u - I_t$; $I_{ct} \equiv I_c - I_t$. The unitary condition, $V_{ub} V_{uq'}^* + V_{cb} V_{cq'}^* + V_{tb} V_{tq'}^* = 0$ with $q' = d$ or s , has been used to achieve the expression. The decay width is $\Gamma = \frac{|\vec{p}|}{8\pi M_{B_c}^2} \sum_{\text{pol}} |\mathcal{M}|^2$, where \vec{p} is the 3-momentum of one of the final state particles in the rest frame of B_c . Generally the amplitude can be written as

$$\mathcal{M} = V_{cb} V_{cq'}^* T_1 + V_{ub} V_{uq'}^* T_2. \quad (12)$$

The amplitude for CP conjugated process can be obtained by conjugating the CKM matrix elements but not T_1 and T_2 , *i.e.* $\bar{\mathcal{M}} = V_{cb}^* V_{cq'} T_1 + V_{ub}^* V_{uq'} T_2$.

The CP asymmetry is defined as

$$\mathcal{A}_{cp} = \frac{\Gamma(B_c^+ \rightarrow \bar{f}) - \Gamma(B_c^- \rightarrow f)}{\Gamma(B_c^+ \rightarrow \bar{f}) + \Gamma(B_c^- \rightarrow f)}. \quad (13)$$

Inserting the expression of the amplitude, one can get

$$\mathcal{A}_{cp} = \frac{\sum \left[2i \text{Im}(T_1 T_2^*) \left(\frac{V_{ub} V_{uq'}^*}{V_{cb} V_{cq'}^*} - \left(\frac{V_{ub} V_{uq'}^*}{V_{cb} V_{cq'}^*} \right)^* \right) \right]}{\sum \left[2|T_1|^2 + 2 \left| \frac{V_{ub} V_{uq'}^*}{V_{cb} V_{cq'}^*} \right|^2 |T_2|^2 + 2 \text{Re}(T_1 T_2^*) \left(\frac{V_{ub} V_{uq'}^*}{V_{cb} V_{cq'}^*} + \left(\frac{V_{ub} V_{uq'}^*}{V_{cb} V_{cq'}^*} \right)^* \right) \right]} \dots \quad (14)$$

In the Wolfenstein parameterization of CKM matrix, up to the λ^3 order, only V_{ub} has weak phase, so we take $\gamma \equiv \arg\left(-\frac{V_{ub}^* V_{ud}}{V_{cb}^* V_{cd}}\right) \simeq \arg\left(\frac{V_{ub}^* V_{us}}{V_{cb}^* V_{cs}}\right)$. Then the CP asymmetry drops to a simple form:

$$\begin{aligned} \mathcal{A}_{cp} &= \frac{\epsilon_i 2 \sum \text{Im}(T_1 T_2^*) \sin \gamma}{\sum |T_1|^2 / B_i + B_i \sum |T_2|^2 + \epsilon_i 2 \sum \text{Re}(T_1 T_2^*) \cos \gamma} \\ &\equiv D_1 \frac{\sin \gamma}{1 + D_2 \cos \gamma}, \quad (15) \end{aligned}$$

where $\epsilon_1 = +1, \epsilon_2 = -1$ corresponding to $B_1 = \left| \frac{V_{ub} V_{us}^*}{V_{cb} V_{cs}^*} \right|, B_2 = \left| \frac{V_{ub} V_{ud}^*}{V_{cb} V_{cd}^*} \right|$.

In our calculation, we take numerical values of CKM elements as [22]

$$\begin{aligned} |V_{ud}| &= 0.97425, & |V_{us}| &= 0.2252, & |V_{ub}| &= 3.89 \times 10^{-3}, \\ |V_{cd}| &= 0.230, & |V_{cb}| &= 0.0406, & |V_{cs}| &= 0.97345. \end{aligned} \quad (16)$$

For current quark masses and QCD coupling constant, we take [4] $(m_u, m_d, m_s, m_c, m_b, m_t) = (0.005, 0.01, 0.175, 1.35, 4.8, 176)$ (GeV) and $\alpha_s(m_b) = 0.235$.

3 The Salpeter method and the model calculation

To estimate the decay rates and CP asymmetries, the hadron matrix elements need to be calculated. In our work, we use the Salpeter method [23], which is the relativistic instantaneous approximation of the Bethe-Salpeter (B-S) equation, with well defined wave functions to deal with the hadron matrix elements.

The B-S equation [24] is written as

$$(\not{p}_1 - m_1)\chi_p(q)(\not{p}_2 + m_2) = i \int \frac{d^4k}{(2\pi)^4} V(P, k, q)\chi_p(k), \quad (17)$$

where $\chi_p(q)$ is B-S wave function of the relevant bound state. P is the four momentum of the state and p_1, p_2, m_1, m_2 are the momenta and constituent masses of the quark and anti-quark, respectively. From the definition

$$\begin{aligned} p_1 &= \alpha_1 P + q, & \alpha_1 &\equiv \frac{m_1}{m_1 + m_2}, \\ p_2 &= \alpha_2 P - q, & \alpha_2 &\equiv \frac{m_2}{m_1 + m_2}, \end{aligned}$$

one can deduce the expression of relative momentum between quark and anti-quark q . $V(P, k, q)$ is the interaction kernel which can be treated as a potential after doing instantaneous approximation, *i.e.* the kernel takes the simple form (in the rest frame)

$$V(P, k, q) \Rightarrow V(|\vec{k} - \vec{q}|).$$

For convenience, we divide the relative momentum q into two parts,

$$q^\mu = q_{\parallel}^\mu + q_{\perp}^\mu, \quad q_{\parallel}^\mu \equiv P \cdot q / M^2 P^\mu, \quad q_{\perp}^\mu \equiv q^\mu - q_{\parallel}^\mu,$$

where M is the mass of the meson. Correspondingly, we have two Lorentz invariant variables:

$$q_P \equiv P \cdot q / M, \quad q_T \equiv \sqrt{-q_{\perp}^2}.$$

With the definitions

$$\varphi_P(q_\perp^\mu) \equiv i \int \frac{dq_P}{2\pi} \chi_P(q_\parallel^\mu, q_\perp^\mu), \quad \eta(q_\perp^\mu) \equiv \int \frac{dk_\perp^3}{(2\pi)^3} V(k_\perp, q_\perp) \varphi_P(q_\perp^\mu),$$

and after performing the integration over q_P in Eq. (17), the B-S equation can be written as

$$\varphi_P(q_\perp) = \frac{\Lambda_1^+(q_\perp) \eta(q_\perp) \Lambda_2^+(q_\perp)}{M - \omega_1 - \omega_2} - \frac{\Lambda_1^-(q_\perp) \eta(q_\perp) \Lambda_2^-(q_\perp)}{M + \omega_1 + \omega_2}, \quad (18)$$

where $\omega_1 = \sqrt{m_1^2 + q_T^2}$, $\omega_2 = \sqrt{m_2^2 + q_T^2}$, and Λ_1^\pm , Λ_2^\pm are the generalized projection operators,

$$\Lambda_1^\pm(q_\perp) \equiv \frac{1}{2\omega_1} \left[\frac{\mathcal{P}}{M} \omega_1 \pm (m_1 + \not{q}_\perp) \right], \quad \Lambda_2^\pm(q_\perp) \equiv \frac{1}{2\omega_2} \left[\frac{\mathcal{P}}{M} \omega_2 \mp (m_2 + \not{q}_\perp) \right].$$

Now we introduce the notations

$$\varphi_P^{\pm\pm}(q_\perp) \equiv \Lambda_1^\pm(q_\perp) \frac{\mathcal{P}}{M} \varphi_P(q_\perp) \frac{\mathcal{P}}{M} \Lambda_2^\pm(q_\perp).$$

With these notations the full Salpeter equation can be written as

$$\begin{aligned} (M - \omega_1 - \omega_2) \varphi_P(q_\perp)^{++} &= \Lambda_1^+(q_\perp) \eta(q_\perp) \Lambda_2^+(q_\perp), \\ (M + \omega_1 + \omega_2) \varphi_P(q_\perp)^{--} &= -\Lambda_1^-(q_\perp) \eta(q_\perp) \Lambda_2^-(q_\perp), \\ \varphi_P(q_\perp)^{+-} &= 0, \quad \varphi_P(q_\perp)^{-+} = 0. \end{aligned} \quad (19)$$

In our model, the Cornell potential, which is a linear scalar interaction plus a vector interaction, is chosen as the instantaneous interaction kernel V .

In solving the equations, the constituent quark masses are taken as

$$m_u = 0.305 \text{ GeV}, \quad m_d = 0.311 \text{ GeV}, \quad m_s = 0.5 \text{ GeV}, \quad m_c = 1.62 \text{ GeV}, \quad m_b = 4.96 \text{ GeV}.$$

The form of wave functions with certain quantum numbers $J^{P(C)} = 0^{-(+)}, 1^{(-)}, 0^{+(+)}, 1^{+(+)}$ and $1^{+(-)}$ ¹ are written as

$$\begin{aligned} \varphi_{0^{-(+)}}(q_\perp) &= M \left[\frac{\mathcal{P}}{M} a_1(q_\perp) + a_2(q_\perp) + \frac{\not{q}_\perp}{M} a_3(q_\perp) + \frac{\mathcal{P} \not{q}_\perp}{M^2} a_4(q_\perp) \right] \gamma_5, \\ \varphi_{1^{-(+)}}(q_\perp) &= (q_\perp \cdot \epsilon_\perp^\lambda) \left[b_1(q_\perp) + \frac{\mathcal{P}}{M} b_2(q_\perp) + \frac{\not{q}_\perp}{M} b_3(q_\perp) + \frac{\mathcal{P} \not{q}_\perp}{M^2} b_4(q_\perp) \right] + M \not{\epsilon}_\perp^\lambda b_5(q_\perp) \\ &\quad + \not{\epsilon}_\perp^\lambda \mathcal{P} b_6(\vec{6}) + (\not{q}_\perp \not{\epsilon}_\perp^\lambda - q_\perp \cdot \epsilon_\perp^\lambda) b_7(q_\perp) + \frac{1}{M} (\mathcal{P} \not{\epsilon}_\perp^\lambda \not{q}_\perp - \mathcal{P} q_\perp \cdot \epsilon_\perp^\lambda) b_8(q_\perp), \\ \varphi_{0^{+(+)}}(q_\perp) &= f_1(q_\perp) \not{q}_\perp + f_2(q_\perp) \frac{\mathcal{P} \not{q}_\perp}{M} + f_3(q_\perp) M + f_4(q_\perp) \mathcal{P}, \\ \varphi_{1^{+(+)}}(q_\perp) &= i \varepsilon_{\mu\nu\alpha\beta} \mathcal{P}^\nu q_\perp^\alpha \epsilon_\perp^{\lambda\beta} \left[g_1(q_\perp) M \gamma^\mu + g_2(q_\perp) \mathcal{P} \gamma^\mu + g_3(q_\perp) \not{q}_\perp \gamma^\mu \right. \\ &\quad \left. + i g_4(q_\perp) \varepsilon^{\mu\rho\sigma\delta} \mathcal{P}_\sigma q_{\perp\rho} \gamma_\delta \gamma_5 / M \right] / M^2, \\ \varphi_{1^{+(-)}}(q_\perp) &= q_\perp \cdot \epsilon_\perp^\lambda \left[h_1(q_\perp) + h_2(q_\perp) \frac{\mathcal{P}}{M} + h_3(q_\perp) \not{q}_\perp + h_4(q_\perp) \frac{\mathcal{P} \not{q}_\perp}{M^2} \right] \gamma_5, \end{aligned} \quad (20)$$

¹ J^P for general particles, J^{PC} for quarkonium *i.e.* the equal mass system. The wave functions satisfy the correct C -parity spontaneously when the masses of quark and anti-quark are equal.

where $a_i(q_\perp), b_i(q_\perp), f_i(q_\perp), g_i(q_\perp)$ and $h_i(q_\perp)$ are wave functions to q_\perp^2 ; M is the mass of corresponding bound state; ϵ_\perp^λ is the polarization vector for $J^P = 1^\pm$ state. With these wave functions, we solve the Salpeter equation (Eq. (19)) and get

$$\begin{aligned} M_{\bar{D}^0} &= 1.865, & M_{D^-} &= 1.869, & M_{D_s^-} &= 1.968, & M_{\eta_c} &= 2...980, \\ M_{\bar{D}^{*0}} &= 2.006, & M_{D^{*-}} &= 2.011, & M_{D_s^{*-}} &= 2.112, & M_{J/\Psi} &= 3.097, \\ M_{\bar{D}_0^{*0}} &= 2.317, & M_{D_0^{*-}} &= 2.323, & M_{D_{s0}^{*-}} &= 2.318, & M_{\chi_{c0}} &= 3.415, \\ M_{\chi_{c1}} &= 3.510, & M_{h_c} &= 3.526, & M_{D_{s1}^-(2460)} &= 2.459, & M_{D_{s1}^-(2536)} &= 2.535, \end{aligned}$$

and $M_{B_c} = 6.276$ in unit of GeV. In our method, the wave functions are constructed for certain J^{PC} quantum state, such as χ_{c1} , which is a $J^{PC} = 1^{++}$ state and also a $^{2s+1}L_J = {}^3P_1$ state and h_c which is a 1^{+-} or 1P_1 state. This is the case for quarkonium. For the particles composed of a couple of quark and anti-quark with different masses, the two states are just 3P_1 and 1P_1 states and both are $J^P = 1^+$ states (such states don't have C-parity), so the mixture between the 3P_1 and 1P_1 states may happen. If one puts the quark masses equal, the two states are spontaneously deduced to 1^{++} and 1^{+-} states respectively. The particles $D_{s1}^-(2460)$ and $D_{s1}^-(2536)$ are considered to be mixed of 3P_1 and 1P_1 states. In this work we take the mixing relation as

$$|P_1^{1/2}\rangle = -\frac{1}{\sqrt{3}}|{}^1P_1\rangle + \sqrt{\frac{2}{3}}|{}^3P_1\rangle, \quad |P_1^{3/2}\rangle = \sqrt{\frac{2}{3}}|{}^1P_1\rangle + \frac{1}{\sqrt{3}}|{}^3P_1\rangle,$$

where $|P_1^{1/2}\rangle$ corresponds to the $D_{s1}^-(2460)$ and $|P_1^{3/2}\rangle$ corresponds to the $D_{s1}^-(2536)$. Interested reader can find details about the Salpeter method and our model in Ref. [25].

With the wave functions of bound states, we can calculate hadron matrix elements, such as $\langle\eta_c|(\bar{c}b)_{V-A}|B_c^-\rangle\langle D^-|(\bar{d}c)_{V-A}|0\rangle$. According to Mandelstam formalism [26], at the leading order, the transition matrix element can be written as [27]

$$\langle\eta_c|(\bar{c}\Gamma^\mu b)|B_c^-\rangle = \int \frac{d^3q_\perp}{(2\pi)^3} \text{Tr} \left[\bar{\varphi}_{\eta_c}^{++}(q_\perp + \alpha'_2 P'_\perp) \Gamma^\mu \varphi_{B_c^-}^{++}(q_\perp) \frac{P}{M} \right], \quad (21)$$

where $\Gamma^\mu = \gamma^\mu(1 - \gamma_5)$; P and M is the momentum and mass of initial state, *i.e.* the B_c meson; P' is the momentum of η_c and $P'_\perp = \frac{P \cdot P}{M^2} P$; $\alpha'_2 = \frac{m_c}{m_c + m_c}$; and $\bar{\varphi}_{\eta_c}^{++} = \gamma_0 \varphi_{\eta_c}^{++} \gamma_0$. The $\langle D^- | (\bar{d}c)_{V-A} | 0 \rangle$ is just a decay constant. For $J^P = 0^\pm$ and 1^\pm particles, we define decay constants f_{0^\pm} and f_{1^\pm} as

$$\langle P(0^\pm) | (\bar{q}_1 q_2)_{V-A} | 0 \rangle \equiv i f_{0^\pm} P^\mu, \quad (22)$$

$$\langle P(1^\pm) | (\bar{q}_1 q_2)_{V-A} | 0 \rangle \equiv i f_{1^\pm} M \epsilon^\mu. \quad (23)$$

Accordingly the transition matrix elements can be expressed with form factors:

$$\langle P'(0^\pm) | (\bar{q}_1 q_2)_{V-A} | P(B_c^-) \rangle \equiv f_+(P + P')^\mu + f_-(P - P')^\mu, \quad (24)$$

$$\langle P'(1^\pm) | (\bar{q}_1 q_2)_{V-A} | P(B_c^-) \rangle \equiv f_1 \frac{\epsilon \cdot P}{M} P^\mu + f_2 \frac{\epsilon \cdot P}{M} P'^\mu + f_3 \epsilon^\mu + i f_4 \epsilon^{\mu\nu} \epsilon^{PP'}, \quad (25)$$

Table 1: Decay constants used in our calculation in unit of MeV.

f_{π^-}	f_{k^-}	f_{D^+}	$f_{D_s^+}$	f_{ρ}	f_{k^*}	f_{ϕ}	f_{D^*}	$f_{D_s^*}$
130 [22]	156 [22]	207 [22]	258 [22]	205 [28]	217 [28]	231 [28]	245 [29]	272 [29]
$f_{J/\Psi}$	f_{η_c}	$f_{D_0^*}$	$f_{D_{s0}^*}$	$f_{D_{s1}(2360)}$	$f_{D_{s1}(2536)}$	$f_{\chi_{c0}}$	$f_{\chi_{c1}}$	f_{h_c}
409[30]	420	137	109	227	77.3	0	239	0

where f_{\pm} and f_i ($i = 1, 2, 3, 4$) are form factors. After all the hadron matrix can be expressed in the products of decay constants and form factors.

4 Numerical results and discussions

We now use the method previously illustrated to estimate the non-leptonic two-body decay widths of B_c meson and their CP asymmetries. In our calculation the decay constants are taken from experimental values or Lattice QCD results, if available. Otherwise, we use the values shown in Table 1.

The decay widths of $B_c^- \rightarrow \eta_c(J/\Psi) + X^-$ for general values of the Wilson coefficients a_1 and a_2 are tabulated in Table 2 compared with the results from other models. We can see that the results from different models are roughly comparable. In our calculation the penguin contributions are shown explicitly keeping the weak phase free. Then it is easy to say that the CP violation arises from the interference between the term with $e^{-i\gamma}$, which is the penguin contribution, and the terms without it, which are dominated by the tree contribution.

The decay widths of $B_c^- \rightarrow \chi_{c0}/\chi_{c1}/h_c + X^-$ for general values of the Wilson coefficients a_1 , a_2 and weak phase γ are shown in Table 3. For $B_c^- \rightarrow \chi_{c0}/h_c + X^-$ decay, the contribution from the color-suppressed diagram is vanished due to the zero decay constants of χ_{c0} and h_c , so the a_1 term dominates the decay width. But this is not true for the decay $B_c^- \rightarrow \chi_{c1} + X^-$. We can see from the table that the numerical factors in front of a_2 are about several times as the factors in front of a_1 , and because the Wilson coefficients are usually taken as $a_1 = 1.14$, $a_2 = -0.20$ [30], the two terms are in the same order and may cancel each other a lot. It means that in this case the decay widths are largely suppressed and may cover effective contributions from the penguin diagrams.

The decay width of B_c^- decaying into a heavy meson (\bar{D}, D^-, \dots) and a light meson (π, K, \dots) are shown in Table 4. In these decay channels, either the color-favored tree diagram or the color-suppressed tree diagram contributes. It can be seen from the table that the penguin diagram contribution is in the leading order as the tree contribution in decays $B_c^- \rightarrow \bar{D}_{(0)}^{(*0)} + K^{(*)-}$. For the decays $B_c^- \rightarrow D_{(0)}^{*-} + \pi^0/\rho^0$, noticing $a_2 \simeq -0.2$, one can find that the penguin effects are as

Table 2: The decay widths of $B_c^- \rightarrow \eta_c(J/\Psi) + X^-$ in the unit of 10^{-15} GeV for general values of the Wilson coefficients a_1, a_2 and weak phase γ .

Final States	Ours	Hernández <i>et. al.</i> [14]	Hady <i>et. al.</i> [7]	Ivanov <i>et. al.</i> [13]
$\eta_c + D^-$	$ 0.438a_1 + 0.290a_2 - (0.0487 - 0.0174i) + (0.0185 - 0.00770i)e^{-i\gamma} ^2$	$(0.438a_1 + 0.236a_2)^2$	$(0.485a_1 + 0.528a_2)^2$	$(0.562a_1 + 0.582a_2)^2$
$\eta_c + D^{*-}$	$ 0.431a_1 + 0.329a_2 - (0.0196 - 0.00681i) + (0.00673 - 0.00305i)e^{-i\gamma} ^2$	$(0.390a_1 + 0.136a_2)^2$	$(0.466a_1 + 0.452a_2)^2$	$(0.511a_1 + 0.310a_2)^2$
$\eta_c + D_0^{*-}$	$ 0.293a_1 + 0.289a_2 - (0.0458 - 0.0149i) + (0.0156 - 0.00691i)e^{-i\gamma} ^2$			
$J/\psi + D^-$	$ 0.371a_1 + 0.258a_2 - (0.00273 - 0.000978i) + (0.00113 - 0.000432i)e^{-i\gamma} ^2$	$(0.328a_1 + 0.156a_2)^2$	$(0.372a_1 + 0.338a_2)^2$	$(0.462a_1 + 0.277a_2)^2$
$J/\psi + D_0^{*-}$	$ 0.212a_1 + 0.273a_2 + (0.00307 - 0.00100i) - (0.00105 - 0.000463i)e^{-i\gamma} ^2$			
$\eta_c + D_s^-$	$ 2.32a_1 + 1.81a_2 - (0.259 - 0.0909i) - (0.00471 - 0.00221i)e^{-i\gamma} ^2$	$(2.54a_1 + 1.93a_2)^2$	$(2.16a_1 + 2.57a_2)^2$	$(2.73a_1 + 2.82a_2)^2$
$\eta_c + D_s^{*-}$	$ 1.98a_1 + 1.82a_2 - (0.0909 - 0.0309i) - (0.00177 - 0.000764i)e^{-i\gamma} ^2$	$(1.84a_1 + 1.17a_2)^2$	$(2.03a_1 + 2.16a_2)^2$	$(2.29a_1 + 1.51a_2)^2$
$\eta_c + D_{s0}^{*-}$	$ 0.987a_1 + 1.34a_2 - (0.169 - 0.0550i) - (0.00320 - 0.00139i)e^{-i\gamma} ^2$			
$\eta_c + D_{s1}^-(2460)$	$ 1.45a_1 + 1.70a_2 - (0.0691 - 0.0218i) - (0.00129 - 0.000561i)e^{-i\gamma} ^2$			
$\eta_c + D_{s1}^-(2536)$	$ 0.475a_1 - 1.59a_2 - (0.0227 - 0.00704i) - (0.000450 - 0.000183i)e^{-i\gamma} ^2$			
$J/\psi + D_s^-$	$ 1.92a_1 + 1.52a_2 - (0.0151 - 0.00528i) - (0.000274 - 0.000129i)e^{-i\gamma} ^2$	$(1.85a_1 + 1.23a_2)^2$	$(1.62a_1 + 1.72a_2)^2$	$(2.19a_1 + 1.32a_2)^2$
$J/\psi + D_{s0}^{*-}$	$ 0.714a_1 + 1.29a_2 + (0.0163 - 0.00531i) + (0.000309 - 0.000134i)e^{-i\gamma} ^2$			

Table 3: The decay widths of $B_c^- \rightarrow \chi_{c0}/\chi_{c1}/h_c + X^-$ in the unit of 10^{-15} GeV for general values of the Wilson coefficients a_1, a_2 and weak phase γ .

Final States	Ours
$\chi_{c0} + D^-$	$ 0.193a_1 - (0.00142 - 0.000508i) + (0.000587 - 0.000224i)e^{-i\gamma} ^2$
$\chi_{c0} + D^{*-}$	$ 0.224a_1 - (0.0101 - 0.00353i) + (0.00349 - 0.00158i)e^{-i\gamma} ^2$
$\chi_{c0} + D_0^{*-}$	$ 0.109a_1 + (0.00158 - 0.000514i) - (0.000538 - 0.000238i)e^{-i\gamma} ^2$
$h_c + D^-$	$ 0.292a_1 - (0.0325 - 0.0116i) + (0.0135 - 0.00514i)e^{-i\gamma} ^2$
$h_c + D^{*-}$	$ 0.290a_1 - (0.0131 - 0.00458i) + (0.00453 - 0.00205i)e^{-i\gamma} ^2$
$h_c + D_0^{*-}$	$ 0.131a_1 - (0.0205 - 0.00668i) + (0.00699 - 0.00309i)e^{-i\gamma} ^2$
$\chi_{c1} + D^-$	$ 0.0465a_1 + 0.173a_2 - (0.00516 - 0.00185i) + (0.00214 - 0.000817i)e^{-i\gamma} ^2$
$\chi_{c1} + D_0^{*-}$	$ 0.0217a_1 + 0.164a_2 - (0.00339 - 0.00110i) + (0.00116 - 0.000511i)e^{-i\gamma} ^2$
$\chi_{c0} + D_s^-$	$ 0.991a_1 - (0.00779 - 0.00273i) - (0.000142 - 0.0000665i)e^{-i\gamma} ^2$
$\chi_{c0} + D_s^{*-}$	$ 1.00a_1 - (0.0460 - 0.0157i) - (0.000898 - 0.000387i)e^{-i\gamma} ^2$
$\chi_{c0} + D_{s0}^{*-}$	$ 0.367a_1 + (0.00837 - 0.00273i) + (0.000159 - 0.0000689i)e^{-i\gamma} ^2$
$\chi_{c0} + D_{s1}^-(2460)$	$ 0.631a_1 - (0.0300 - 0.00946i) - (0.000559 - 0.000243i)e^{-i\gamma} ^2$
$\chi_{c0} + D_{s1}^-(2536)$	$ 0.192a_1 - (0.00917 - 0.00284i) - (0.000181 - 0.0000739i)e^{-i\gamma} ^2$
$h_c + D_s^-$	$ 1.46a_1 - (0.163 - 0.0572i) - (0.00297 - 0.00139i)e^{-i\gamma} ^2$
$h_c + D_s^{*-}$	$ 1.26a_1 - (0.0580 - 0.0197i) - (0.00113 - 0.000487i)e^{-i\gamma} ^2$
$h_c + D_{s0}^{*-}$	$ 0.445a_1 - (0.0761 - 0.0248i) - (0.00144 - 0.000627i)e^{-i\gamma} ^2$
$h_c + D_{s1}^-(2460)$	$ 0.716a_1 - (0.0340 - 0.0107i) - (0.000635 - 0.000276i)e^{-i\gamma} ^2$
$h_c + D_{s1}^-(2536)$	$ 0.214a_1 - (0.0103 - 0.00318i) - (0.000203 - 0.0000827i)e^{-i\gamma} ^2$
$\chi_{c1} + D_s^-$	$ 0.232a_1 + 0.930a_2 - (0.0259 - 0.00909i) - (0.000471 - 0.000221i)e^{-i\gamma} ^2$
$\chi_{c1} + D_{s0}^{*-}$	$ 0.0740a_1 + 0.716a_2 - (0.0127 - 0.00412i) - (0.000240 - 0.000104i)e^{-i\gamma} ^2$

Table 4: The decay widths of $B_c^- \rightarrow D + \text{light meson}$ in the unit of 10^{-15} GeV for general values of the Wilson coefficients a_1 , a_2 and weak phase γ .

Final States	Ours	Choi <i>et. al.</i> [16]
$\bar{D}^0 + K^-$	$ (0.00425a_1 - (0.000286 - 0.000116i))e^{-i\gamma} - (0.0156 - 0.00367i) ^2$	$(0.00625a_1)^2$
$\bar{D}^0 + K^{*-}$	$ (0.00621a_1 - (0.000267 - 0.000108i))e^{-i\gamma} - (0.0143 - 0.00367i) ^2$	$(0.00866a_1)^2$
$\bar{D}^{*0} + K^-$	$ (0.00614a_1 - (0.000115 - 0.0000466i))e^{-i\gamma} - (0.00629 - 0.00148i) ^2$	
$\bar{D}^{*0} + K^{*-}$	$ (0.00942a_1 - (0.000404 - 0.000164i))e^{-i\gamma} - (0.0217 - 0.00556i) ^2$	
$\bar{D}_0^{*0} + K^-$	$ (0.00401a_1 - (0.0000753 - 0.0000304i))e^{-i\gamma} - (0.00411 - 0.000966i) ^2$	
$\bar{D}_0^{*0} + K^{*-}$	$ (0.00594a_1 - (0.000255 - 0.000103i))e^{-i\gamma} - (0.0137 - 0.00351i) ^2$	
$\bar{D}^0 + \pi^-$	$ (0.0150a_1 - (0.000983 - 0.000404i))e^{-i\gamma} + (0.00284 - 0.000794i) ^2$	$(0.0217a_1)^2$
$\bar{D}^0 + \rho^-$	$ (0.0249a_1 - (0.00108 - 0.000434i))e^{-i\gamma} + (0.00308 - 0.000838i) ^2$	$(0.0374a_1)^2$
$\bar{D}^{*0} + \pi^-$	$ (0.0219a_1 - (0.000422 - 0.000174i))e^{-i\gamma} + (0.00122 - 0.000341i) ^2$	
$\bar{D}^{*0} + \rho^-$	$ (0.0374a_1 - (0.00162 - 0.000652i))e^{-i\gamma} + (0.00462 - 0.00126i) ^2$	
$\bar{D}_0^{*0} + \pi^-$	$ (0.0141a_1 - (0.000272 - 0.000112i))e^{-i\gamma} + (0.000787 - 0.000220i) ^2$	
$\bar{D}_0^{*0} + \rho^-$	$ (0.0238a_1 - (0.00103 - 0.000415i))e^{-i\gamma} + (0.00294 - 0.000801i) ^2$	
$D^- + \pi^0$	$ (0.0108a_2 + (0.000649 - 0.000260i))e^{-i\gamma} - (0.00183 - 0.000511i) ^2$	$(0.0155a_2)^2$
$D^- + \rho^0$	$ (0.0181a_2 + (0.000764 - 0.000315i))e^{-i\gamma} - (0.00223 - 0.000608i) ^2$	$(0.0265a_2)^2$
$D^{*-} + \pi^0$	$ (0.0157a_2 + (0.000424 - 0.000170i))e^{-i\gamma} - (0.00119 - 0.000333i) ^2$	
$D^{*-} + \rho^0$	$ (0.0270a_2 + (0.00114 - 0.000470i))e^{-i\gamma} - (0.00333 - 0.000908i) ^2$	
$D_0^{*-} + \pi^0$	$ (0.0102a_2 + (0.000275 - 0.000110i))e^{-i\gamma} - (0.000774 - 0.000216i) ^2$	
$D_0^{*-} + \rho^0$	$ (0.0171a_2 + (0.000723 - 0.000297i))e^{-i\gamma} - (0.00211 - 0.000575i) ^2$	

large as the tree diagram contributions. So one can expect these channels have sufficiently large CP asymmetries.

To estimate numerical values of decay rates and CP asymmetries, we now take $a_1 = 1.14$ and $a_2 = -0.2$ [16, 30]. For the weak phase, we use the relation $\gamma = \arg(\bar{\rho} + i\bar{\eta})$ and take the value $\bar{\rho} = 0.132$, $\bar{\eta} = 0.341$ [22], which give $\gamma = 1.20$ (68.8°). The lifetime $\tau_{B_c} = 0.46$ [31] is used to calculate the decay branching ratio. Taking these values we calculate branching ratios and CP asymmetries of non-leptonic two-body B_c decay which are shown in Table 5 and Table 6. In the tables, D_1 and D_2 are defined in Eq. (15); $\epsilon_f N$ in the last column are the numbers of B_c^\pm events needed for testing CP violation. For three standard deviation (3σ) signature $\epsilon_f N \sim \frac{9}{Br \mathcal{A}_{cp}^2}$, where ϵ_f is the detecting efficiency of the final state.

The channels of B_c decaying into two heavy mesons *i.e.* a charmonium and a D or D_s meson are listed in Table 5. These decays are dominated by the tree diagrams, and only for CP violation, the penguin diagram effects arise through the interference with the tree diagram. The decay ratios of the processes with a D meson (channels 1-15) in the final state are generally smaller than those with a D_s meson (channels 16-40), since in the former processes the tree diagrams have CKM factor $V_{cb}V_{cd}^*$ which is of order λ^3 while in the processes (16-40) the tree diagrams have CKM factor $V_{cb}V_{cs}^* \sim \lambda^2$, where $\lambda = 0.2253$ [22] is a Wolfenstein parameter. The CP asymmetries in the channels (1-15) are generally larger than those in (16-40). In order to

Table 5: The CP asymmetries and branching ratios of B_c non-leptonic decays [I]. D_1 and D_2 are defined as $\mathcal{A}_{CP} \equiv D_1 \frac{\sin \gamma}{1 + D_2 \cos \gamma}$, where γ is the weak phase (see Eq. (15)); $\epsilon_f N$ are the numbers of B_c^\pm events needed for testing CP violation at three standard deviation (3σ) level, which are decided by $\epsilon_f N \sim \frac{9}{Br \mathcal{A}_{cp}^2}$, where ϵ_f is the detecting efficiency of the final state. The following values are taken in calculation: $a_1 = 1.14$, $a_2 = -0.2$ and weak phase $\gamma = 68.8^\circ$. For channels with $\eta_c, J/\Psi$ and χ_{c1} , color-favored tree, color-suppressed tree and penguin diagrams contribute; for channels with χ_{c0} and h_c only color-favored tree and penguin diagrams contribute due to the zero decay constants of the χ_{c0} and h_c .

No.	Final States	D_1	D_2	\mathcal{A}_{cp}	$Br(B_c^+ \rightarrow f)$	$Br(B_c^- \rightarrow f)$	$\epsilon_f N$
1	$\eta_c + D^-$	0.0432	0.0920	0.0390	1.16×10^{-4}	1.07×10^{-4}	5.30×10^7
2	$\eta_c + D_0^{*-}$	0.0680	0.130	0.0605	4.18×10^{-5}	3.70×10^{-5}	6.23×10^7
3	$\eta_c + D^{*-}$	0.0155	0.0329	0.0143	1.19×10^{-4}	1.15×10^{-4}	3.76×10^8
4	$\chi_{c0} + D^-$	0.00207	0.00538	0.00192	3.34×10^{-5}	3.33×10^{-5}	7.30×10^{10}
5	$\chi_{c0} + D_0^{*-}$	-0.00375	-0.00859	-0.00351	1.09×10^{-5}	1.10×10^{-5}	6.66×10^{10}
6	$\chi_{c0} + D^{*-}$	0.0133	0.0283	0.0123	4.29×10^{-5}	4.18×10^{-5}	1.41×10^9
7	$h_c + D^-$	0.0375	0.0879	0.0339	6.77×10^{-5}	6.33×10^{-5}	1.20×10^8
8	$h_c + D_0^{*-}$	0.0532	0.105	0.0477	1.27×10^{-5}	1.16×10^{-5}	3.25×10^8
9	$h_c + D^{*-}$	0.0133	0.0283	0.0123	7.21×10^{-5}	7.03×10^{-5}	8.38×10^8
10	$\chi_{c1} + D^-$	0.161	0.292	0.135	1.62×10^{-7}	1.23×10^{-7}	3.45×10^9
11	$\chi_{c1} + D_0^{*-}$	-0.0681	-0.205	-0.0686	8.14×10^{-8}	9.33×10^{-8}	2.19×10^{10}
12	$\chi_{c1} + D^{*-}$	0.0178	0.0373	0.0164	2.62×10^{-5}	2.54×10^{-5}	1.30×10^9
13	$J/\psi + D^-$	0.00236	0.00613	0.00219	9.55×10^{-5}	9.51×10^{-5}	1.96×10^{10}
14	$J/\psi + D_0^{*-}$	-0.00482	-0.0111	-0.00451	2.50×10^{-5}	2.52×10^{-5}	1.76×10^{10}
15	$J/\psi + D^{*-}$	0.0156	0.0329	0.0143	3.23×10^{-4}	3.14×10^{-4}	1.37×10^8
16	$\eta_c + D_s^-$	-0.00239	-0.00455	-0.00223	2.860×10^{-3}	2.873×10^{-3}	6.30×10^8
17	$\eta_c + D_{s0}^-$	-0.00474	-0.00891	-0.00443	3.322×10^{-4}	3.352×10^{-4}	1.37×10^9
18	$\eta_c + D_s^{*-}$	-0.000881	-0.00195	-0.000821	2.273×10^{-3}	2.276×10^{-3}	5.87×10^9
19	$\eta_c + D_{s1}^-(2460)$	-0.000933	-0.00205	-0.000870	1.091×10^{-3}	1.093×10^{-3}	1.09×10^{10}
20	$\eta_c + D_{s1}^-(2536)$	-0.000447	-0.00107	-0.000416	4.900×10^{-4}	4.904×10^{-4}	1.06×10^{11}
21	$\chi_{c0} + D_s^-$	-0.000119	-0.000252	-0.000111	8.802×10^{-4}	8.804×10^{-4}	8.28×10^{11}
22	$\chi_{c0} + D_{s0}^-$	0.000318	0.000746	0.000297	1.273×10^{-4}	1.272×10^{-4}	8.04×10^{11}
23	$\chi_{c0} + D_s^{*-}$	-0.000728	-0.00163	-0.000679	8.412×10^{-4}	8.423×10^{-4}	2.32×10^{10}
24	$\chi_{c0} + D_{s1}^-(2460)$	-0.000728	-0.00161	-0.000679	3.320×10^{-4}	3.325×10^{-4}	5.88×10^{10}
25	$\chi_{c0} + D_{s1}^-(2536)$	-0.000730	-0.00172	-0.000680	3.057×10^{-5}	3.062×10^{-5}	6.35×10^{11}
26	$h_c + D_s^-$	-0.00200	-0.00387	-0.00187	1.576×10^{-3}	1.581×10^{-3}	1.63×10^9
27	$h_c + D_{s0}^-$	-0.00328	-0.00651	-0.00306	1.298×10^{-4}	1.306×10^{-4}	7.36×10^9
28	$h_c + D_s^{*-}$	-0.000728	-0.00163	-0.000679	1.336×10^{-3}	1.338×10^{-3}	1.46×10^{10}
29	$h_c + D_{s1}^-(2460)$	-0.000728	-0.00161	-0.000679	4.278×10^{-4}	4.284×10^{-4}	4.56×10^{10}
30	$h_c + D_{s1}^-(2536)$	-0.000730	-0.00172	-0.000680	3.827×10^{-5}	3.832×10^{-5}	5.08×10^{11}
31	$\chi_{c1} + D_s^-$	-0.0112	-0.0160	-0.0105	1.964×10^{-6}	2.005×10^{-6}	4.14×10^{10}
32	$\chi_{c1} + D_{s0}^-$	0.00252	0.00686	0.00234	3.609×10^{-6}	3.592×10^{-6}	4.56×10^{11}
33	$\chi_{c1} + D_s^{*-}$	-0.000995	-0.00218	-0.000928	4.919×10^{-4}	4.928×10^{-4}	2.12×10^{10}
34	$\chi_{c1} + D_{s1}^-(2460)$	-0.00108	-0.00235	-0.00101	1.761×10^{-4}	1.764×10^{-4}	5.01×10^{10}
35	$\chi_{c1} + D_{s1}^-(2536)$	-0.000633	-0.00150	-0.000591	4.259×10^{-5}	4.264×10^{-5}	6.05×10^{11}
36	$J/\psi + D_s^-$	-0.000139	-0.000293	-0.000129	2.432×10^{-3}	2.432×10^{-3}	2.21×10^{11}
37	$J/\psi + D_{s0}^-$	0.000458	0.00108	0.000427	2.299×10^{-4}	2.297×10^{-4}	2.15×10^{11}
38	$J/\psi + D_s^{*-}$	-0.000884	-0.00196	-0.000824	6.752×10^{-3}	6.764×10^{-3}	1.96×10^9
39	$J/\psi + D_{s1}^-(2460)$	-0.000875	-0.00192	-0.000817	5.339×10^{-3}	5.348×10^{-3}	2.53×10^9
40	$J/\psi + D_{s1}^-(2536)$	-0.000639	-0.00151	-0.000596	1.123×10^{-3}	1.124×10^{-3}	2.26×10^{10}

Table 6: The CP asymmetries and branching ratios of B_c non-leptonic decays [II]. D_1 and D_2 are defined as $\mathcal{A}_{CP} \equiv D_1 \frac{\sin \gamma}{1 + D_2 \cos \gamma}$, where γ is the weak phase (see Eq. (15)); $\epsilon_f N$ are the numbers of B_c^\pm events needed for testing CP violation at three standard deviation (3σ) level, which are decided by $\epsilon_f N \sim \frac{9}{Br \mathcal{A}_{cp}^2}$, where ϵ_f is the detecting efficiency of the final state. The following values are taken in calculation: $a_1 = 1.14$, $a_2 = -0.2$ and weak phase $\gamma = 68.8^\circ$. Color-favored tree and penguin diagrams contribute in the channels (41-52); color-suppressed tree and penguin diagrams contribute in the channels (59-64); for the other channels in this table, only penguin diagram contributes.

No.	Final States	D_1	D_2	\mathcal{A}_{cp}	$B_r(B_c^+ \rightarrow f)$	$B_r(B_c^- \rightarrow f)$	$\epsilon_f N$
41	$\bar{D}^0 + K^-$	0.133	-0.509	0.152	1.83×10^{-7}	1.34×10^{-7}	2.44×10^9
42	$\bar{D}^0 + K^{*-}$	0.201	-0.735	0.255	1.70×10^{-7}	1.01×10^{-7}	1.02×10^9
43	$\bar{D}^{*0} + K^-$	0.235	-0.970	0.338	5.41×10^{-8}	2.68×10^{-8}	1.95×10^9
44	$\bar{D}^{*0} + K^{*-}$	0.201	-0.735	0.255	3.91×10^{-7}	2.32×10^{-7}	4.44×10^8
45	$\bar{D}_0^{*0} + K^-$	0.235	-0.970	0.338	2.31×10^{-8}	1.14×10^{-8}	4.57×10^9
46	$\bar{D}_0^{*0} + K^{*-}$	0.201	-0.735	0.255	1.56×10^{-7}	9.23×10^{-8}	1.11×10^9
47	$\bar{D}^0 + \pi^-$	-0.104	0.338	-0.0861	1.93×10^{-7}	2.30×10^{-7}	5.75×10^9
48	$\bar{D}^0 + \rho^-$	-0.0640	0.221	-0.0552	5.41×10^{-7}	6.04×10^{-7}	5.15×10^9
49	$\bar{D}^{*0} + \pi^-$	-0.0285	0.0992	-0.0256	4.25×10^{-7}	4.47×10^{-7}	3.15×10^{10}
50	$\bar{D}^{*0} + \rho^-$	-0.0640	0.221	-0.0552	1.22×10^{-6}	1.36×10^{-6}	2.29×10^9
51	$\bar{D}_0^{*0} + \pi^-$	-0.0285	0.0992	-0.0256	1.77×10^{-7}	1.86×10^{-7}	7.56×10^{10}
52	$\bar{D}_0^{*0} + \rho^-$	-0.0640	0.221	-0.0552	4.93×10^{-7}	5.51×10^{-7}	5.65×10^9
53	$D^- + K^0$	0.00593	0.0375	0.00545	1.91×10^{-7}	1.89×10^{-7}	1.60×10^{12}
54	$D^- + K^{*0}$	0.00576	0.0363	0.00530	1.60×10^{-7}	1.58×10^{-7}	2.01×10^{12}
55	$D^{*-} + K^0$	0.00593	0.0375	0.00545	3.20×10^{-8}	3.16×10^{-8}	9.52×10^{12}
56	$D^{*-} + K^{*0}$	0.00576	0.0363	0.00530	3.71×10^{-7}	3.68×10^{-7}	8.68×10^{11}
57	$D_0^{*-} + K^0$	0.00593	0.0375	0.00545	1.36×10^{-8}	1.35×10^{-8}	2.24×10^{13}
58	$D_0^{*-} + K^{*0}$	0.00576	0.0363	0.00530	2.72×10^{-7}	2.70×10^{-7}	1.18×10^{12}
59	$D^- + \pi^0$	-0.419	0.884	-0.296	3.88×10^{-9}	7.14×10^{-9}	1.87×10^{10}
60	$D^- + \rho^0$	-0.359	0.909	-0.252	9.44×10^{-9}	1.58×10^{-8}	1.13×10^{10}
61	$D^{*-} + \pi^0$	-0.248	0.713	-0.184	6.42×10^{-9}	9.31×10^{-9}	3.39×10^{10}
62	$D^{*-} + \rho^0$	-0.359	0.909	-0.252	2.11×10^{-8}	3.52×10^{-8}	5.05×10^9
63	$D_0^{*-} + \pi^0$	-0.248	0.713	-0.184	2.70×10^{-9}	3.92×10^{-9}	8.07×10^{10}
64	$D_0^{*-} + \rho^0$	-0.359	0.909	-0.252	8.43×10^{-9}	1.41×10^{-8}	1.26×10^{10}
65	$D_s^- + K^0$	-0.0593	-0.650	-0.0723	2.19×10^{-8}	2.54×10^{-8}	7.27×10^{10}
66	$D_s^- + K^{*0}$	-0.0747	-0.633	-0.0904	1.90×10^{-8}	2.28×10^{-8}	5.28×10^{10}
67	$D_{s0}^{*-} + K^0$	-0.0593	-0.650	-0.0723	1.03×10^{-9}	1.19×10^{-9}	1.55×10^{12}
68	$D_{s0}^{*-} + K^{*0}$	-0.0747	-0.633	-0.0904	1.08×10^{-8}	1.30×10^{-8}	9.25×10^{10}
69	$D_s^{*-} + K^0$	-0.0593	-0.650	-0.0723	3.22×10^{-9}	3.73×10^{-9}	4.95×10^{11}
70	$D_s^{*-} + K^{*0}$	-0.0747	-0.633	-0.0904	3.75×10^{-8}	4.50×10^{-8}	2.67×10^{10}
71	$D_{s1}^-(2460) + K^0$	-0.0593	-0.650	-0.0723	3.75×10^{-8}	4.34×10^{-8}	4.25×10^{10}
72	$D_{s1}^-(2460) + K^{*0}$	-0.0747	-0.633	-0.0904	3.68×10^{-8}	4.41×10^{-8}	2.72×10^{10}
73	$D_{s1}^-(2536) + K^0$	-0.0593	-0.650	-0.0723	3.61×10^{-8}	4.17×10^{-8}	4.43×10^{10}
74	$D_{s1}^-(2536) + K^{*0}$	-0.0747	-0.633	-0.0904	3.15×10^{-8}	3.77×10^{-8}	3.18×10^{10}
75	$D_s^- + \phi^0$	0.00422	0.0414	0.00387	5.19×10^{-7}	5.15×10^{-7}	1.16×10^{12}
76	$D_{s0}^{*-} + \phi^0$	0.00422	0.0414	0.00387	3.02×10^{-7}	3.00×10^{-7}	1.99×10^{12}
77	$D_s^{*-} + \phi^0$	0.00422	0.0414	0.00387	1.05×10^{-6}	1.04×10^{-6}	5.73×10^{11}
78	$D_{s1}^-(2460) + \phi^0$	0.00422	0.0414	0.00387	1.08×10^{-6}	1.07×10^{-6}	5.56×10^{11}
79	$D_{s1}^-(2536) + \phi^0$	0.00422	0.0414	0.00387	8.65×10^{-7}	8.59×10^{-7}	6.95×10^{11}

test the CP violating effects, we need both branching ratio and CP asymmetry to be sufficiently large. It is shown in the Table 5 that the most favorite channels are $B_c^- \rightarrow \eta_c + D^- / D_0^{*-}$.

In Table 6, we show that color-favored tree and penguin diagrams contribute in the channels (41-52); color-suppressed tree and penguin diagrams contribute in the channels (59-64); for the other channels in this table, only penguin diagram contributes. As discussed before, in the amplitudes of the processes (41-46) and (59-64), the tree contribution and the penguin contribution are in the same order, so only (47-52) are tree dominated processes. The branching ratios in Table 6 are generally smaller than those in Table 5: It is because (i) the tree amplitudes (if exist) in the channels of Table 6 are Cabibbo suppressed due to the small magnitude of V_{ub} , and (ii) most of the form factors for the decays listed in Table 6 are smaller than those in Table 5.

The processes (41-46) and (59-64) have significantly large CP asymmetries. The CP violating effects are mainly coming from the interference between the tree diagram and the penguin diagram. Since the branching ratios of these decays are small, the numbers of B_c for testing CP effects are around $10^9 \sim 10^{10}$, which may be too large for LHC experiments.

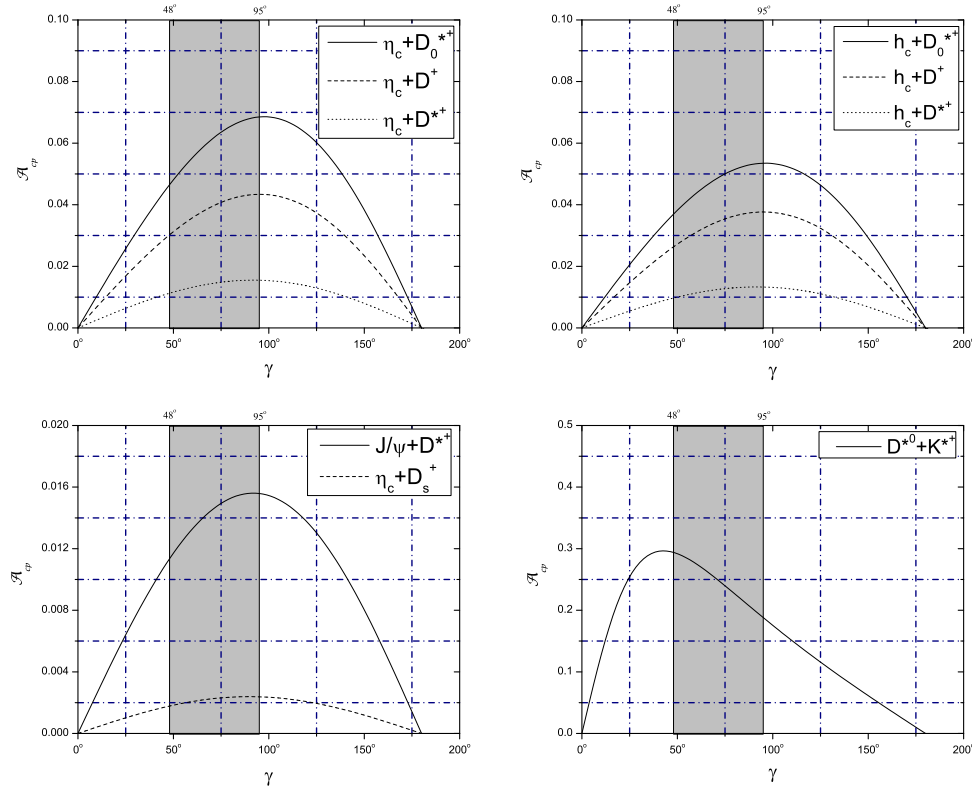


Figure 2: Dependence of the CP asymmetries \mathcal{A}_{CP} upon the weak phase γ in a few interesting processes. The shaded region is the constrained range of γ measured in tree level B decay, which is about $48^\circ \sim 95^\circ$.

Table 7: The branching ratios and CP asymmetries of a few interesting channels at different k^2 , where k is the momentum of gluon in the QCD loop integrals (see Eqs. (3-5)).

k^2	$B_r(B_c^+ \rightarrow f)$				\mathcal{A}_{CP}			
	$0.35m_b^2$	$0.50m_b^2$	$0.65m_b^2$	$0.80m_b^2$	$0.35m_b^2$	$0.50m_b^2$	$0.65m_b^2$	$0.80m_b^2$
$\eta_c + D^+$	1.09×10^{-4}	1.13×10^{-4}	1.15×10^{-4}	1.16×10^{-4}	0.0383	0.0391	0.0389	0.0387
$\eta_c + D_0^{*+}$	3.89×10^{-5}	4.10×10^{-5}	4.20×10^{-5}	4.27×10^{-5}	0.0593	0.0609	0.0605	0.0599
$\eta_c + D^{*+}$	1.16×10^{-4}	1.18×10^{-4}	1.18×10^{-4}	1.19×10^{-4}	0.0142	0.0143	0.0143	0.0143
$h_c + D^+$	6.41×10^{-5}	6.59×10^{-5}	6.69×10^{-5}	6.75×10^{-5}	0.0332	0.0338	0.0337	0.0335
$h_c + D_0^{*+}$	1.20×10^{-5}	1.25×10^{-5}	1.28×10^{-5}	1.30×10^{-5}	0.0469	0.0480	0.0477	0.0473
$h_c + D^{*+}$	7.08×10^{-5}	7.16×10^{-5}	7.20×10^{-5}	7.23×10^{-5}	0.0122	0.0123	0.0123	0.0123
$J/\psi + D^{*+}$	3.17×10^{-4}	3.21×10^{-4}	3.23×10^{-4}	3.24×10^{-4}	0.0143	0.0144	0.0144	0.0143
$\eta_c + D_s^+$	2.69×10^{-3}	2.79×10^{-3}	2.84×10^{-3}	2.88×10^{-3}	-0.00223	-0.00226	-0.00225	-0.00223
$D^{*0} + K^{*+}$	4.02×10^{-7}	3.85×10^{-7}	3.66×10^{-7}	3.51×10^{-7}	0.142	0.279	0.342	0.383

According to Table 5 and 6, the $\epsilon_f N$ of the decays $B_c^- \rightarrow \eta_c + D^-/D_0^{*-}$ are of order $\sim 10^7$ and the values for the processes B_c^- decaying into $\eta_c + D^{*-}/D_s^-$, $h_c + D^-/D^{*-}/D_0^{*-}$, $J/\Psi + D^{*-}$ and $\bar{D}^{*0} + K^{*-}$ are of order $\sim 10^8$. Since the LHC-b is expected to produce around 5×10^{10} B_c events per year, they are hopeful channels to be tested for the CP violation. In Fig. 2, we draw the CP asymmetry *vs* the weak phase of these channels to see their dependence on γ using Eq. (15). The shaded region is the constrained range of γ measured in tree level B decay, which is $48^\circ \sim 95^\circ$ [22]. From the figure we can see the CP asymmetries of these processes may suffer about $\sim 30\%$ uncertainty. Fortunately the Global fit of the Wolfenstein parameters provided a more rigorous constraint for the weak phase γ .

In calculating the QCD loop integrals we take the gluon momentum k by using Eq. (5). For the processes in Table 5, k^2 is estimated to be around $(0.6 \sim 0.7)m_b^2$, and for the processes in Table 6, k^2 to be around $(0.4 \sim 0.5)m_b^2$. Eq. (5) is based on a simple kinematic picture, but it is too simple to reflect the final state hadronization dynamics. So we investigate how much it will affect the CP asymmetry and decay rate if the value of k^2 varies. The branching ratios and CP asymmetries of most interested channels at different k^2 are shown in Table 7. According to the table, the branching ratios of all the channels are barely affected by k^2 . For CP asymmetries, only the CP asymmetry of $B_c^- \rightarrow \bar{D}^{*0} + K^{*-}$ process is sensitive to the value of k^2 . Actually we find that the branching ratios of all the channels calculated are barely affected by the value of k^2 , and so are the CP asymmetries of processes (1-40), but the CP asymmetries of processes (41-79) are sensitive to k^2 .

In summary, we calculated the decay rates and CP asymmetries of non-leptonic two-body decay of B_c meson. Based on our calculation we have found that the best decay channels to observe CP violation at LHC are $B_c^- \rightarrow \eta_c + D^-/D_0^{*-}$. Decays to $\eta_c + D^{*-}/D_s^-$, $h_c + D^-/D^{*-}/D_0^{*-}$, $J/\Psi + D^{*-}$ are also hopeful channels. In this work the soft strong phases are

not calculated, which may cause uncertainty of the results and need further study.

Acknowledgments

The work of C.S.K. was supported in part by the Basic Science Research Program through the NRF of Korea funded by MOEST (2009-0088395) and in part by KOSEF through the Joint Research Program (F01-2009-000-10031-0). The work of G.W. was supported in part by the National Natural Science Foundation of China (NSFC) under Grant No. 10875032 and supported in part by Projects of International Cooperation and Exchanges NSFC under Grant No. 10911140267.

References

- [1] F. Abe *et al.*, (CDF Collaboration), Phys. Rev. D 58, (1998) 112004; Phys. Rev. Lett. 81,(1998) 2432.
- [2] I. P. Gouz, V.V. Kiselev, A. K. Likhoded, V. I. Romanovsky, and O. P. Yushchenko, Phys. At. Nucl. 67, (2004) 1559-1570; Yad. Fiz. 67, (2004) 1581-1592.
- [3] C-H. Chang, and Y-Q. Chen, Phys. Rev. D 49, (1994) 3399-3411.
- [4] J-F. Liu. and K-T. Chao. Phys. Rev. D56, (1997) 4133.
- [5] A. Anisimov, P. Y. Kulikov, I. M. Narodetskii and K. A. Ter-Martirosyan, Phys. Atom. Nucl. 62, (1999) 1739-1753; Yad. Fiz. 62, (1999) 1868-1882.
- [6] Y-S. Dai and D-S. Du. Eur. Phys. J. C 9, (1999) 557-564.
- [7] A. A. El-Hady, J. H. Muñoz and J. P. Vary, Phys. Rev. D 62, (2000) 014019.
- [8] P. Colangelo and F. D. Fazio, Phys. Rev. D 61, (2000) 034012.
- [9] R. Fleischer and D. Wyler, Phys. Rev. D 62, (2000) 057503.
- [10] D. Ebert, R. N. Faustov and V. O. Galkin, Phys. Rev. D 68, (2003) 094020; Eur. Phys. J. C 32, (2003) 29-43; Phys. Rev. D 82, (2010) 034019.
- [11] M. A. Ivanov, J. G. Körner and O. N. Pakhomova, Phys. Lett. B 555, (2003) 189-196.
- [12] V. V. Kiselev, J. Phys. G 30, (2004) 1445-1457; arXiv:hep-ph/0308214 (2003); arXiv:hep-ph/0211021 (2003).

- [13] M. A. Ivanov, J. G. Körner and P. Santorelli, Phys. Rev. D 73, (2006) 054024.
- [14] E. Hernández, J. Nieves and J. M. Verde-Velasco, Phys. Rev. D 74, (2006) 074008.
- [15] J-F. Sun, Y-L. Yang, W-J. Du and H-L. Ma, Phys. Rev. D 77, (2008) 114004.
- [16] H-M. Choi and C-R Ji, Phys. Rev. D 80, (2009) 114003.
- [17] G. Buchalla, A. J. Buras and M. E. Lautenbacher, Rev. Mod. Phys. 68, (1996) 1125-1244;
A. J. Buras, hep-ph/9806471, (1998).
- [18] D-S. Du. and Z-Z. Xing. Phys. Rev. D 48, (1993) 4155-4162.
- [19] J-M Gérard and W-S. Hou, Phys. Rev. Lett. 62, (1989) 855-858; Phys. Rev. D 43, (1991) 2909-2930.
- [20] A. Ali and C. Greub, Phys. Rev. D 57, (1998) 2996-3016.
- [21] M. Neubert and B. Stech, Adv. Ser. Direct. High Energy Phys. 15, (1998) 294-344.
- [22] K. Nakamura *et al.* (Particle Data Group), J. Phys. G 37, (2010) 075021.
- [23] E. E. Salpeter, Phys. Rev. 87, (1952) 328.
- [24] E. E. Salpeter, H. A. Bethe, Phys. Rev. 84, (1951) 1232.
- [25] C. S. Kim, G-L. Wang, Phys. Lett. B 584, (2004) 285; G-L. Wang, Phys. Lett. B 633, (2006) 492; G-L. Wang, Phys. Lett. B 650 (2007) 15-21; C-H. Chang, G-L. Wang, Sci. China G 53, (2010) 2025-2030.
- [26] S. Mandelstam, Proc. R. Soc. London 233 (1955) 245.
- [27] C-H. Chang, C.S. Kim and G-L. Wang, Phys. Lett. B 623, (2005) 218-226; C-H. Chang, J-K. Chen. and G-L. Wang, Commun. Theor. Phys. 46, (2006) 467-480.
- [28] P. Ball and R. Zwicky, Phys. Rev. D 71, (2005) 014029.
- [29] D. Becirevic *et al.* Phys. Rev. D 60, (1999) 074501.
- [30] N. Brambilla. *et al.* (Quarkonium Working Group). CERN Yellow Report, CERN-2005-005.
- [31] A. Abulencia *et al.*(CDF Collaboration), Phys. Rev. Lett. 97, (2006) 012002 ; T. Aaltonen *et al.*(CDF Collaboration), Phys. Rev. Lett. 100, (2008) 182002.

